Gas-phase vibrational spectra of glyoxylic acid and its gem diol monohydrate. Implications for atmospheric chemistry

ARTICLE *in* REACTION KINETICS AND CATALYSIS LETTERS · APRIL 2009

Impact Factor: 0.93 · DOI: 10.1007/s11144-009-5528-2

Jointly published by
Akadémiai Kiadó, Budapest
and Springer, Dordrecht

React.Kinet.Catal.Lett.
Vol. 96, No. 2, 209–224 (2009)
10.1007/s11144-009-5528-2

RKCL5528

GAS-PHASE VIBRATIONAL SPECTRA OF GLYOXYLIC ACID AND ITS GEM DIOL MONOHYDRATE. IMPLICATIONS FOR ATMOSPHERIC CHEMISTRY

Kathryn L. Plath[a,b], Jessica L. Axson[a,b], Galen C. Nelson[a], Kaito Takahashi[a], Rex T. Skodje[a] and Veronica Vaida[a,b]*

[a]Department of Chemistry and Biochemistry, Campus Box 215, University of Colorado Boulder, CO 80309, USA

[b]CIRES, Campus Box 215, University of Colorado, Boulder, CO 80309, USA

Received February 2, 2009, in revised form February 6, 2009, accepted February 6, 2009

Abstract

The interconversion of aldehydes and ketones to geminal diols in the presence of water impacts the role of oxidized organics in the atmosphere. While this equilibrium has been noted in condensed phases, we provide experimental evidence of it in the gas-phase. Glyoxylic acid and its geminal diol counterpart are observed in the gas-phase and their fundamental vibrational spectra were assigned and analyzed for the effects of intra- and intermolecular hydrogen bonding. The IR spectra are used to probe the differences in their structures and hydrogen bonding tendencies.

Keywords: glyoxylic acid, atmospheric organic aerosols, vibrational spectroscopy

INTRODUCTION

Highly oxidized organic molecules, in particular aldehydes and ketones, have a unique and complex role in water uptake and aerosol formation in the atmosphere. These compounds are found in the highly oxidized material of secondary organic aerosols (SOA) [1-9]. Aldehydes, and to a lesser extent ketones, are known to form a gem diol in the presence of water [10, 11]. The gem diol drastically changes the physical and chemical properties of the molecules, which impacts the partitioning between gas and particle phase as well as the chemistry of such molecules in the atmosphere. The conversion of

* Corresponding author. Tel.: (303) 492-1422; Fax: (303) 492-5894
E-mail: Vaida@colorado.edu

0133-1736/2009/US$ 20.00.

glyoxylic acid (GA) to the diol form of glyoxylic acid monohydrate (GAM), 2,2-dihydroxyacetic acid, is heavily influenced by the presence of water. Due to the gem diol's tendency to form strong intermolecular hydrogen bonds, it will partition predominantly to the condensed phase. The aldehyde form of glyoxylic acid also has the ability to form hydrogen bonds; however it has a much higher vapor pressure and is more likely to remain in the gas-phase than its diol analogue. Both GA and GAM have several rotational conformers that are populated at temperatures less than 100˚ C [12-14]. Using these two molecules and their many conformers the effects of inter- and intramolecular hydrogen-bonding are studied to understand the water mediated equilibrium between the aldehyde and diol forms of glyoxylic acid and its environmental implications [15, 16].

Intramolecular hydrogen bonds can have a large impact on the physical and chemical properties of a molecule. One interesting case of intramolecular hydrogen bonding is that of geminal diols due to the increased strain imposed by the two alcohol groups on a single carbon. The gem diol is well-known in aqueous solution through NMR investigations [10, 11, 17], however to the best of our knowledge, it has not been observed in the gas-phase in any system. The gem diol forms intermolecular hydrogen bonds consequently lowering the vapor pressure compared to the carbonyl analogues. The readiness of GA to form the diol GAM diminishes the presence of GA in the gas-phase and may explain the discrepancy between atmospheric model predictions of the abundance of aldehydes and ketones in the atmosphere and results of field measurements of such molecules [18]. We present the first recorded gas-phase IR spectrum of a gem diol, GAM, along with a reinvestigation of the IR spectrum of GA. Varying the experimental conditions allows us to better understand the gas-phase equilibrium of GA and GAM. Intramolecular hydrogen bonds cause shifts in the vibrational modes, primarily in the OH stretching mode and carbonyl stretching mode. These shifts have a typical magnitude of <100 cm^{-1}. In contrast, intermolecular hydrogen bonds cause larger shifts (200 – 500 cm^{-1}) in the vibrational spectrum. By altering the experimental conditions it is also possible to probe the strength of the intermolecular hydrogen bonds, which provides insight into a molecule's tendency to form aggregates.

GA has been studied as a simple difunctionalized organic compound. The microwave spectrum provided the geometry for GA [13, 14]. A theoretical investigation of the rotamers and intramolecular hydrogen bonding [12] previously discussed its ability to form hydrogen bond. Spectroscopically, GA was recorded in the IR in gas-phase and matrix environments, along with CCl_4 solutions [19-21]. The electronic state photochemical unimolecular reactions have been studied both theoretically and experimentally [22, 12]. The GAM has been recorded by NMR spectroscopy [23], however it has not been seen in the gas-phase. The rate constant for dehydration of aldehyde hydrates has been discussed, including the equilibrium between GA and GAM in aqueous phase

[24, 25]. The work of Sorenson *et. al.* found that the equilibrium constant favors the GAM over GA [25]. While gem diols have been observed in aqueous solutions, they have been postulated to exist in the gas-phase, but never observed. Due to their ability to form intermolecular hydrogen bonds they would have a low vapor pressure, yet by careful control of the experimental conditions we observe the gem diol in the gas-phase.

Diols with alcohol groups on separate carbons are stable and their vibrational spectroscopy has been studied previously [26-28]. The spectroscopic work on diols provides an excellent opportunity to study the difference between intramolecular hydrogen bonded alcohol groups and free alcohol groups. Gem diols are expected to engage in intramolecular hydrogen bonding similar to other diols. If aldehydes and ketones form diols as readily in the atmosphere as has been seen in the laboratory, then our current treatment of these compounds in atmospheric models does not accurately describe their behavior. This may be the cause of the discrepancy between atmospheric field measurements of aldehydes and ketones and the values derived from atmospheric models [18].

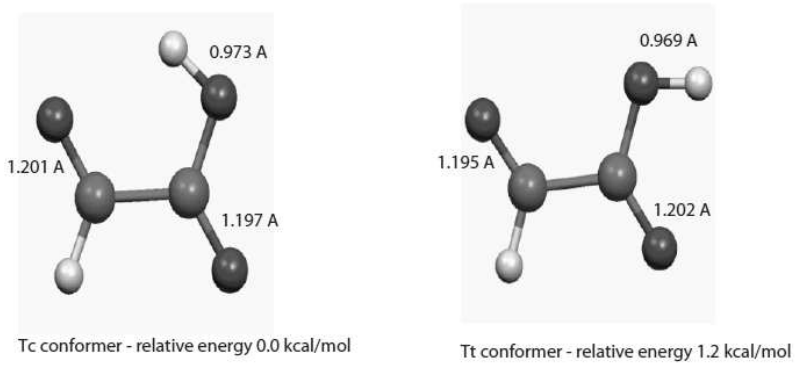

Fig. 1. Calculated structures for the two lowest energy conformers of GA. Several bond lengths are included to highlight differences relating to the OH bond

EXPERIMENTAL SECTION

Sample preparation

GA (HCOCOOH, 98%) was purchased from Sigma-Aldrich. It exists as the monohydrate due to its large hydrophilicity and is comprised almost completely of the diol form ($HC(OH)_2COOH$), 2,2-dihydroxyacetic acid. In order to

increase the population of GA relative to GAM the sample needed to be processed and dried. The difficulty associated with this issue has been noted in nearly all experimental studies of glyoxylic acid [19-22, 25, 29, 30]. Activated molecular sieves were added to the sample and sealed at ambient conditions for 5-7 days. The sample was attached to a vacuum line (~30 millitorr) and gently heated to 313 K for 12 – 48 hours. This method produced the cleanest sample of the aldehyde, however any introduction of water to the sample quickly formed the diol. GA has a higher vapor pressure than GAM and was easier to observe in the gas-phase. These vapor pressures are not known values. Throughout the experiment both forms existed, but we were able to exert some control over their relative populations by changing the temperature, flow rate, and relative humidity. Relative populations can be estimated using the peak intensities of transitions that are assigned to each substance. The aldehyde and diol forms were distinguishable by the difference in melting points. As an aldehyde, GA melts at ~318 K; however, in GAM the melting point rises greatly to ~343 K. We suggest this is proof of the GAM's tendency to form intermolecular hydrogen bonds.

Fourier Transform Infra-Red Spectra

The mid- infrared absorption spectra of GA and GAM were measured between 800 and 5000 cm^{-1} using FTIR at 370 K and 1 cm^{-1} resolution. A Bruker Tensor 27 with a permanent set-up of a globar, KBR beamsplitter, and MCT detector allowed for optimal mid-IR absorption spectroscopy. The set-up for this experiment has been described previously [31-35]. The glass cell has a path length of 75 cm. N_2 gas was bubbled through a molten sample of GA and GAM to force the sample through the cell. The cell was wrapped in heating tape for temperature control. N_2 gas was also used to create a purge volume between the cooler windows and the hot sample to prevent condensation of the sample. The FTIR technique allows for the simultaneous measurement of all wavelengths of light, producing accurate relative intensities of the various peaks in the fundamental vibrational range. The temperature of the cell varied between 365 and 373 K.

Theoretical calculations

The structures and fundamental vibrational mode frequencies of GA and GAM were calculated using the hybrid density functional theory method of B3LYP [36, 37] with the 6-311++G(3df,3pd) basis set [38-42] using the Gaussian 03 program [40]. The frequencies were scaled using the wavenumber

linear scaling method of Yoshida *et. al.* [43]. The optimized structures with bond lengths are given in Fig. 1 and Fig. 3. The most stable structure (Tc) reveals an intramolecular hydrogen bonding causing the elongation of the O-H bond compared to the Tt conformer. The calculated frequencies and integrated cross-sections are presented in Table 1 and Table 2. Previously, this method calculated the results of pyruvic acid and was in excellent agreement with experimental results and the results obtained with CCSD(T) methods [35, 44].

RESULTS AND DISCUSSION

This work presents the fundamental vibrational spectra of GA and GAM in order to gain insight into the structure of these molecules, their ability to form intra- and inter-molecular hydrogen bonds, their relative vapor pressures, atmospheric aerosol partitioning, and tendency for uptake into water of these molecules. While the IR spectrum of GA has been measured previously in gas-phase [19] this study provides the first IR spectrum of GAM. Theoretical calculations acted as a guide to assign the GAM spectrum. The theoretical structures of GA and GAM elucidated differences in the structures, which are confirmed in the spectral shifts we observed; the structures are presented in Fig. 1 and Fig. 3. The gas-phase vibrational spectrum of GA, which was previously published by Fleury and Tabacik [19], shown in Fig. 2, and Table 1 gives the comparison of our recorded spectrum with the previous work as well as our theoretical results. The GAM spectrum and assignments are available in Fig. 4 and Table 2.

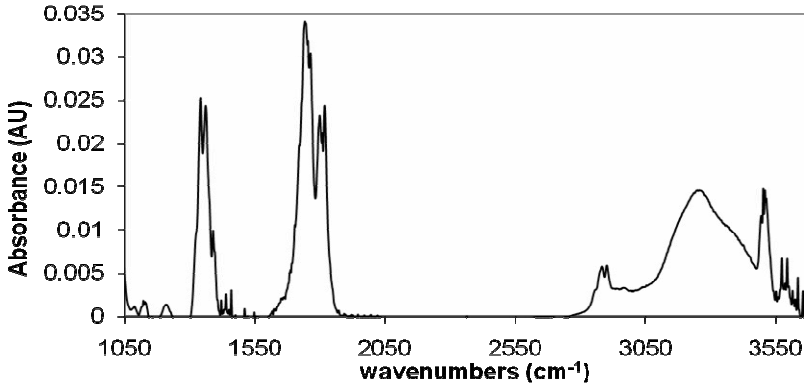

Fig. 2. Fundamental Spectrum of GA. The OH stretching transitions for both the Tc and Tt conformers are observed. The spectrum was collected at 365 K with 1 cm^{-1} resolution

Table 1

The results of the re-examination of the GA spectrum. We present the experimental frequencies, FWHM's, the theoretical frequencies and intensities, and the literature frequencies for the fundamental modes, as well as the mode descriptions

Theoretical Frequency	Experimental Frequency	Literature Frequency[19]	Theoretical Intensity	Experimental FWHM	Mode Descriptions [19]*
164			29.1		CHO torsion (A")
276			33.3		frame bend
493			6.2		C=O bend
568			29.9		COOH torsion (A")
674			76.5		OH outplane bend (A")
676			15.0		frame bend
		773			dCCOacid + dCCO aldehyde
862	896	876	50.0	21	C-C stretch + C-O stretch
	957	948		88	YCC(=H)-O
998	1006		3.6	50	
1184	1206	1205	3.5	36	dCOH + C-O stretch + C-Cstretch
1319	1323	1305	23.4	19.5	C-O stretch + C-C stretch + dCOH
1335	1351	1348	324.5	53	dCCH + dCOH
1749	1751	1755	103.3	68	C=O aldehyde stretch
1791	1807	1809	238.4	22	C=O acid stretch
2881	2878	2860	38.7	51	CH stretch
3490	3501	3510	99.9	45	OH stretch (Tc conformer)
3561	3584		80.5	49	OH stretch (Tt conformer)

* The mode descriptions for transitions less than 700 cm^{-1} are from this paper's theoretical calculations. Mode descriptions for transitions longer than 800 cm-1 are from the work of Fleury and Tabacik [19]

Spectrum of Glyoxylic Acid (GA)

A reexamination of the IR spectrum of GA with our new theoretical results reveals new insight into gas-phase GA (Table 1 and Fig. 2.). In our experiment the thermal energy was sufficient to populate the Tt conformer of GA in addition to the most stable Tc conformer. According to our calculations, the Tt

conformer is 1.2 kcal/mol higher in energy relative to the Tc conformer. The major difference between these two structures is in the orientation of the carboxylic acid group's hydrogen atom. In the Tc conformer the O-H group is oriented toward the aldehyde group creating an intramolecular hydrogen bond. Based on the selected bond lengths shown in Fig. 1, the Tc conformer shows a longer OH bond length compared to the Tt conformer. Using the C=O bond lengths, it appears that in the Tc conformer there is an interaction between the OH group and the aldehyde group, while in the Tt conformer the trend of C=O bond lengths suggests that the OH is interacting with the C=O of the carboxylic acid group. The differences in the C=O bond lengths suggests where the intramolecular interactions occur, however the OH bond length reveals that the intramolecular hydrogen bond in the Tc conformer is stronger than that of the Tt conformer. These structures are reminiscent of those seen in pyruvic acid, where two similar conformers were observed in the gas-phase [12, 35, 44]. From the frequency and intensity changes seen in the vibrational spectrum we can confirm the subtle structural differences and investigate the relative strength of the intramolecular forces.

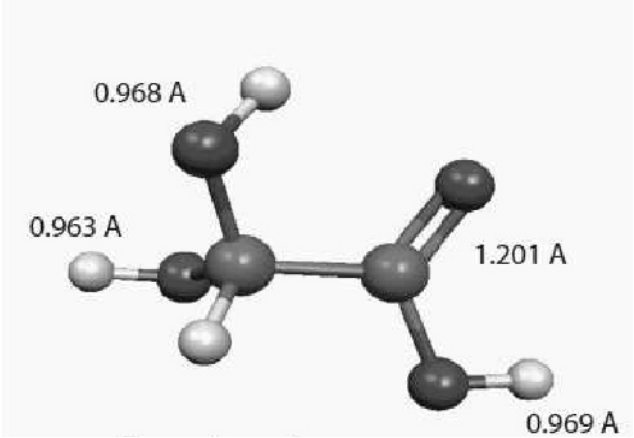

Fig. 3. The calculated structure of the most stable conformer of GAM. Bond lengths are provided for comparison with the GA results

There are several vibrational bands that we identify and assign to GA. At 1351 cm^{-1}, there is a distinct doublet feature that we assign as the GA fundamental C-O stretching mode. This peak is in good agreement with Fleury and Tabacik [19] at 1348 cm^{-1}, and with the calculated position of 1335 cm^{-1}. The theoretical intensity is 324.5 km/mol, which is evident in the strength of this mode. The clear doublet structure of this peak, which is also seen in the Fleury and Tabacik spectrum, is a distinct feature that we use to identify a majority concentration of the aldehyde form of GA in our spectrum [19].

The carbonyl stretches of the molecules are difficult to separate because their frequencies change very little. In GA, the aldehyde C=O stretch is slightly lower in frequency than the C=O of the carboxylic acid functional group, as is the case for pyruvic acid [35, 44]. The aldehyde C=O stretch is assigned at 1751 cm^{-1}. The agreement is good with the Fleury and Tabacik spectrum and our theoretical calculations, 1755 cm^{-1} and 1749 cm^{-1} respectively [19]. The predicted intensity is 103.3 km/mol, which suggests that it would be one of the more intense vibrational modes of GA. The theoretical predictions suggest that the C=O stretch of the carboxylic acid functional group has a larger cross-section, 238.4 km/mol. We assign the C=O stretch of GA's carboxylic acid at 1807 cm^{-1}, in good agreement with the literature (1809 cm^{-1}) and the theoretical calculations 1791 cm^{-1}. The literature assigns this transition as having a PQR structure, and we can confirm the shape in our own spectra. However, in our spectra we observe the lower energy transition with more intensity and a larger linewidth. We attribute this to overlapping transitions of multiple species. One of these overlapping transitions could be the aldehyde carbonyl stretching transition of the Tt conformer of the GA, which should have a slightly blue shifted frequency due to the lack of intramolecular hydrogen bonding that is present in the Tc conformer of GA. Using several data sets, we modeled the two transitions using Gaussian functions and found that a typical function used to fit the peak at 1751 cm^{-1} has a line-width of 65 cm^{-1}, while the peak at 1807 cm^{-1} has a line-width of ~35 cm^{-1}. We use the linewidth as evidence that the lower energy peak is the result of multiple transitions.

The OH stretch of the GA aldehyde is unique and easily assigned. We place the transition at 3501 cm^{-1}. Our theoretical results are 3490 cm^{-1} and 99.9 km/mol, while Fleury and Tabacik assign the OH stretch at 3510 cm^{-1} [19]. At the elevated temperatures of our experiment the Tt conformer is observable; its OH stretch is present at 3584 cm^{-1}. Theoretical predictions place this transition at 3561 cm^{-1}. The predicted intensity is less than that of the Tc conformer (80.5 km/mol), which combined with the lower population, suggests the small intensity of the Tt conformer's OH stretch transition we observe. These results fit the trend of the similar molecule, pyruvic acid, where the OH stretches of the two conformers are separated by 120 cm^{-1} [35, 44]. We attribute the difference in the frequencies to an intramolecular hydrogen bond; this is supported by the calculated structures (in Fig. 1) showing the Tc conformer's longer OH bond compared to the Tt conformer [45].

The spectrum provided by Fleury and Tabacik [19] was invaluable in understanding our spectra; however there are several vibrational mode assignments with which we do not agree. There is a mode at 948 cm^{-1} that Fleury and Tabacik [19] observed, which is not observed in our experimental data or predicted by our calculations. We do not believe that this peak is due to a fundamental transition of glyoxylic acid. It is not predicted in either of the

conformers of GA or in the GAM fundamental transitions. With minor discrepancies, our gas-phase spectra and theoretical results agree well with those obtained by Fleury and Tabacik [19].

Spectrum of the Gem Diol form of Glyoxylic Acid Monohydrate (GAM)

In addition to obtaining and reexamining the IR spectrum of GA, we measured the fundamental spectrum of GAM. To the best of our knowledge, this species has not been seen in the gas-phase before. The results are presented in Table 2 and the spectrum is displayed in Fig. 4. The GAM vibrational modes have several frequencies that are unique and can be used to easily identify the presence of GAM in the spectrum. These occur mainly in the fingerprint region of the spectrum (< 1500 cm^{-1}). We assign the spectrum using the frequencies and intensities from B3LYP calculations reported here. The GA spectrum serves as a calibration for our assignment of this unknown spectrum because GA has a previously published spectrum [19] to compare with our experimental and theoretical results as was done above. The theoretical results and our experimental data reveal a confidence in the vibrational frequency of within 20 cm^{-1}. The agreement between GAM's experimental and theoretical frequencies is within 30 cm^{-1}.

The theoretical results predict that the transition at 1006 cm^{-1} can be attributed to either GAM or GA. In this case, the predicted GA vibrational mode is not recorded by the Fleury and Tabacik paper or in our spectrum [19]. The GA mode is calculated at 998 cm^{-1} with an integrated intensity of 3.6 km/mol. This low intensity may be the reason why no such mode is observed. In our spectrum, shown in Fig. 4, the feature at 1006 cm^{-1} is relatively intense, unlike the calculated intensity for the GA vibrational mode. However, the GAM calculations predict the C-OH stretch vibrational transition centered at 1023 cm^{-1} with an intensity of 142.6 km/mol. This fits much better with the observed data, and as such we make this tentative assignment.

A large feature in the spectrum of the GAM lies at 1101 cm^{-1}. This peak is completely absent from the GA spectrum. Theoretical results place two modes in this vicinity: one at 1079 cm^{-1} with an intensity of 257.4 km/mol and the other at 1148 cm^{-1} and an intensity of 137.7 km/mol. The shape of the peak fits well with the idea that there are multiple transitions contained within it. A shoulder exists to the high energy side of the peak (~1130 cm^{-1}), which we tentatively assign as the higher energy mode predicted at 1148 cm^{-1}.

The feature at 1206 cm^{-1} is present in all spectra regardless of sample composition; however spectra with a large population of GAM reveal this feature relatively larger than in the spectrum of GA. This fits with the calculated intensities: for the GA transition, the calculated frequency of the OH bending

vibrational mode is 1184 cm^{-1} (Fleury and Tabacik [19] assign it at 1205 cm^{-1}) and intensity of 3.5 km/mol, and for GAM a calculated frequency of 1196 cm^{-1} and an intensity of 69.9 km/mol. The combination of experimental spectra and theoretical calculations suggest that two distinct modes belonging to separate molecules overlap and the assignment of a particular peak to one molecule must be done by comparing the intensity to the intensity of peaks of known vibrational modes. Thus, by comparing the intensity of the peak at 1206 cm^{-1} to the intensity of the C=O stretch of the carboxylic acid carbonyl of GA we can assign this feature. If the 1206 cm^{-1} peak is less intense, as is the case in Fig. 2 then the 1206 cm^{-1} feature is due to the GA OH bend vibrational mode. However, in cases where the intensity of the 1206 cm^{-1} transition is equal to or greater than the 1807 cm^{-1} C=O stretch, the feature is the result of the GAM CH bending vibrational mode. This assignment is supported by Fleury and Tabacik's assignment of a feature at 1205 cm^{-1} as the dCOH + C-O stretch + C-C stretch vibrational mode of GA observed with a low intensity in their spectrum [19].

At 1320 cm^{-1} we assign the OH bending mode based on the predicted frequency for the mode at 1314 cm^{-1}. This mode helps to show the majority species in our spectrum due to its proximity to the 1351 cm^{-1} GA vibrational mode. These two transitions are easily distinguishable due to the differing band shapes. The GA doublet is a very strong mode in the spectrum and as we increase the GAM population we see the disappearance of the doublet and the rise of the structureless peak at 1320 cm^{-1}. While the 1351 cm^{-1} transition has a very large calculated intensity (324.5 km/mol) the GAM vibrational mode transition has a much smaller calculated intensity of 77.7 km/mol. This suggests that the population of gas-phase GAM in Fig. 4 is greater than the gas-phase population of GA in Fig. 2.

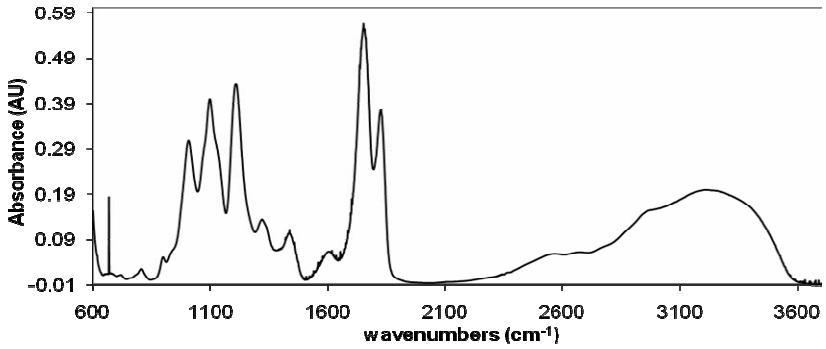

Fig. 4. FTIR spectrum of GAM. The spectrum was collected at 370 K and 1 cm^{-1} resolution. The large broad feature toward high energy represents the OH stretching modes engaged in intermolecular hydrogen bonding

Overlapping of transitions make it difficult to ascertain the absolute peak position for the GAM C=O stretch, however we assign the mode a frequency at 1742 cm^{-1}. The theoretical calculations predict a frequency of 1771 cm^{-1} and an intensity of 291.3 km/mol, which is more intense than the predicted carbonyl stretches of GA. By taking many spectra at different conditions and assigning certain peaks as being uniquely GAM or GA we have data that we believe result from samples with an overwhelming majority of GAM compared to GA. From these spectra we determine the frequency of the carbonyl stretch of the GAM mode. When compared to the carboxylic acid carbonyl stretch of the GA, the GAM C=O stretch is significantly red-shifted, which we attribute to increased hydrogen bonding compared to the carboxylic acid carbonyl of GA, this increased intramolecular interaction results in lessened electron density between the carbon and oxygen atoms. As seen in Fig. 4, the transition centered at 1750 cm^{-1} does not have as clear of a PQR structure as the higher energy transition, however some structure is present. Using the work of Fleury and Tabacik [19], the PQ and RQ branches are observed in our spectra. We also note a third structural feature at 1742 cm^{-1}, which we believe is the GAM C=O stretching mode transition sitting next to and commingled with the GA aldehyde carbonyl stretch. In spectra where the vast majority of the population is in the GAM form the structure of the carbonyl stretches disappear and the 1742 cm^{-1} transition becomes the dominant feature. This larger shift in the GAM C=O stretching frequency compared to the C=O stretching frequency of the carboxylic acid group of glyoxylic acid suggests that the intramolecular hydrogen bond formed in GAM is stronger than that of GA. This is manifested in the theoretical calculations with the longer C=O bond length (1.201 Å).

The OH stretching modes of GAM monomer are not observed with certainty in this spectrum. The predicted frequencies are 3555, 3557, and 3624 cm^{-1}, and the intensities are lower than in GA (75.6, 58.7, and 53.8 km/mol respectively). In the spectrum there is a large broad feature between 3000 cm^{-1} and 3500 cm^{-1}. This type of feature is often seen in spectra of compounds that are known to dimerize or form clusters. The height of the feature scales with the population of GAM in the cell. The broad feature fits with intermolecular hydrogen bonded OH stretching modes. Calculations on the GA: H_2O cluster reveal that the OH group involved in the intermolecular hydrogen bond is red-shifted to 3146 cm^{-1} and the intensity is predicted to be 902 km/mol. We assume there would be a similar result for the GAM: H_2O cluster. This result shows a much larger perturbation to the OH stretching mode than is typically seen in intramolecular hydrogen bonds such as pyruvic acid, GA, or glycolic acid [46, 35]. The low vapor pressure and high melting point of GAM reinforce the concept that GAM forms strong intermolecular interactions. These greatly shifted hydrogen bonded transitions would account for the lack of monomeric GAM OH stretching mode transitions observed.

Table 2

The theoretical and experimental results for the fundamental spectrum of GAM

Theoretical Frequency (cm^{-1})	Experimental Frequency (cm^{-1})	Theoretical Intensity (km/mol)	Experimental FWHM (cm^{-1})	Mode Description
66		1.1		Torsion
222		50.9		OH rock
256		45.1		OH rock
291		32.4		frame bend
390		30.2		OH rock
459		56.6		OH rock
558		61.3		OH rock
593		89.0		OH rock
661		27.5		Torsion
759		54.5		C-C stretch
843		63.6		C-C str+OH bend
1023	1065	142.6		C-OH stretch
1079	1101	257.4	96	C-OH stretch
1148		137.7		C-OH stretch
1196	1206	69.9	46	CH bend
1265		14.1		OH bend
1314	1320	77.7	97	OH bend
1364	1390	30.0	19	CH bend
1452	1434	17.6	65	CH bend
1771	1742	291.3	69	OHC=O stretch
2931		27.1		CH stretch
3555		75.6		OH stretch
3557		58.7		OH stretch
3624		53.8		OH stretch

Proof for hydrated complexes in our experiment is limited, though the increased intensity and large frequency shifts can be observed under the right experimental conditions. Both GA and GAM are prone to forming clusters and

intermolecular hydrogen bonds; GAM appears to form stronger intermolecular interactions than GA. This is consistent with our observation that the melting point of GA is ~315 K and GAM is ~343 K. Additionally, the vapor pressure of GA is predicted to be higher than that of GAM, though it is possible to get a large population of GAM into the vapor phase at ~370 K. In data sets with a large amount of vapor phase water there also exists a feature at 1610 cm^{-1} that we attribute to these hydrated complexes; this feature is shown in Fig. 4. and only observed in spectra that are predominantly GAM. It is impossible to assign this feature to a specific molecule. The peak position is red-shifted from typical C=O stretching frequencies due to a strong hydrogen bond. The water molecule creates a stronger hydrogen bond with GAM because it is not constrained by the geometry of the molecule and thus provokes larger shifts in the spectrum than result from intramolecular hydrogen bonding.

Gas-Phase Equilibrium between GA and GAM

It is evident that the equilibrium between GA and GAM is highly dependent on the water partial pressure and temperature. Using the calculated intensities of transitions in our spectra we can estimate the population ratio of GAM to GA. The GA mode at 1351 cm^{-1} and the GAM transition at 1390 cm^{-1} are observed in all of the collected spectra. Spectra, such as that of Fig. 1, have a large number density of GA, however in our estimation the GAM:GA ratio is ~2. Fig. 4 is a spectrum with a much larger population of GAM, our calculated ratio of GAM:GA is ~500. From these ratios we conclude that the GAM:GA ratio clearly favors GAM to a large extent.

If we assume that the equilibrium is solely due to the gas-phase reaction of the isolated GA and water molecule to form gas-phase GAM then the theoretically calculated free energy change gives an equilibrium constant favoring GA and water. In our results we observe a larger relative population of GAM, implying that the simple assumed equilibrium is not correct in describing the observations. The discrepancy between the calculated equilibrium constant above and the experimentally derived result can be understood with reference to the involvement of hydrogen bonded complexes. Our spectroscopic observations of complexes are evidence that GA and to a larger extent GAM form hydrogen bonded complexes, as discussed above. The complexes must be incorporated into the equilibrium to get an accurate result. We conclude, based on our observed spectra and population ratio estimations, that the gas-phase equilibrium between GAM and GA is water-mediated and involves hydrated complexes of GA and GAM.

Atmospheric Implications

Glyoxylic acid is a known product of the oxidation of glyoxal and is incorporated into atmospheric models [2, 3]. Based on our experiments it appears that at relevant atmospheric conditions GA will become the geminal diol form, GAM, in a short amount of time due to the large amount of water present in the atmosphere [3]. Once GAM forms it is unlikely to remain in the gas-phase and will partition to aerosols and clouds due to its propensity for forming intermolecular hydrogen bonds [47]. This ability to form hydrated clusters affects the molecule's transport and chemistry in the troposphere. We can extrapolate from our experimental results to temperatures relevant to the atmosphere that GAM will have a nearly negligible vapor pressure, though the vapor pressure of GA will still be appreciable. The reaction of GA to form GAM is inevitable if GA partitions to the aerosol. These experiments showed that in the gas-phase the GAM is favored. Following the uptake of GA to the aerosol, the subsequent reaction to form GAM, and the low vapor pressure of GAM ensures that little GA will reappear in the gas-phase. This may account for the discrepancy between the modeled amounts of ketones and aldehydes in the atmosphere and the much lower observed concentrations of these species. In addition to the removal of the aldehyde from the gas-phase, the diol functional group also drastically changes the electronic states. GA has a low lying electronic state that can undergo photochemistry in the troposphere. However, GAM has a higher energy excited electronic state and will thus remain inert to the accessible UV light in the troposphere [29]. As the first reported gas-phase spectrum of a gem diol, this work also highlights the question of how water affects the organic aerosol mass [48]. In the atmosphere, hydration seems to be an additional pathway that shifts the partitioning equilibrium [49]. Additionally the chemistry and contribution to SOA of aldehydes and ketones requires reevaluation in light of these results.

Acknowledgements. The authors would like to thank Barbara Ervens, David DeHaan, and Tad Koch for helpful discussions. V. V. thanks the National Science Foundation and R.T.S. thanks the Petroleum Research Fund for financial support.

REFERENCES

1. A.G. Carlton, B.J. Turpin, K.E. Altieri, S. Seitzinger, A. Reff, H.J. Lim, B. Ervens: *Atmos. Environ.*, **41**, 7588 (2007).
2. B. Ervens, A.G. Carlton, B.J. Turpin, K.E. Altieri, S.M. Kreidenweis, G. Feingold: *Geophys. Res. Lett.*, 35, L02816 (2008).

3. B. Ervens, G. Feingold, G.J. Frost, S.M. Kreidenweis: *J. Geophys. Res. Atmos.*, 109, D15205 (2004).
4. B. Ervens, S. Gligorovski, H. Herrmann: *Phys. Chem. Chem. Phys.*, **5**, 1811 (2003).
5. B. Ervens, S.M. Kreidenweis: *Environ. Sci. Technol.*, **41**, 3904 (2007).
6. M. Kanakidou, J.H. Seinfeld, S.N. Pandis, I. Barnes, F.J. Dentener, M.C. Facchini, R. Van Dingenen, B. Ervens, A. Nenes, C.J. Nielsen, E. Swietlicki, J.P. Putaud, Y. Balkanski, S. Fuzzi, J. Horth, G.K. Moortgat, R. Winterhalter, C.E.L. Myhre, K. Tsigaridis, E. Vignati, E.G. Stephanou, J. Wilson: *Atmos. Chem. Phys.*, **5**, 1053 (2005).
7. C.M. Rosado-Reyes, J.S. Francisco: *J. Phys. Chem. A*, **110**, 4419 (2006).
8. P. Warneck: *J. Atmos. Chem.*, **51**, 119 (2005).
9. M. Hallquist, J.C. Wenger, U. Baltensperger, Y. Rudich, D. Simpson, M. Claeys, J. Dommen, N.M. Donahue, C. George, A.H. Goldstein, J.F. Hamilton, H. Herrmann, T. Hoffmann, Y. Iinuma, M. Jang, M. Jenkin, J.L. Jimenez, A. Kiendler-Scharr, W. Maenhaut, G. McFiggans, T.F. Mentel, A. Monod, A.S.H. Prevot, J.H. Seinfeld, J.D. Surratt, R. Szmigielski, J. Wildt: *Atmos. Chem. Phys.*, **9**, 3555 (2009).
10. D.R. Kent, S.L. Widicus, G.A. Blake, W.A. Goddard: *J. Chem. Phys.*, 119, 5117 (2003).
11. M. Mugnai, G. Cardini, V. Schettino, C.J. Nielsen: *Mol. Phys.*, **105**, 2203 (2007).
12. C. Chen, S.F. Shyu: *J. Mol. Struct. Theochem*, **503**, 201 (2000).
13. K.M. Marstokk, H. Mollenda: *J. Mol. Struct.*, **15**, 137 (1973).
14. B.P. Vaneijck, F.B. Vanduijneveldt: *J. Mol. Struct.*, **39**, 157 (1977).
15. V. Vaida: *J. Phys. Chem. A*, **113**, 5 (2009).
16. V. Vaida, K.J. Feierabend, N. Rontu, K. Takahashi: *Int. J. Photoenergy*, Article ID 138091 (2008).
17. M. Rodler: *Chem. Phys.*, **105,** 345 (1986).
18. R. Volkamer, J.L. Jimenez, F. San Martini, K. Dzepina, Q. Zhang, D. Salcedo, L.T. Molina, D.R. Worsnop, M.J. Molina: *Geophys. Res. Lett.*, 33, L17811 (2006).
19. G. Fleury, V. Tabacik: *J. Mol. Struct.*, **10**, 359 (1971).
20. H. Hollenstein, T.K. Ha, H.H. Gunthard: *J. Mol. Struct.*, **146**, 289 (1986).
21. R.L. Redington, C.K.J. Liang: *J. Mol. Spectr.*, **104**, 25 (1984).
22. C.W. Bock, R.L. Redington: *J. Phys. Chem.*, **92**, 1178 (1988).
23. A.J.L. Cooper, A.G. Redfield: *J. Biol. Chem.*, **250**, 527 (1975).
24. P. George, C.W. Bock, M. Trachtman: *J. Mol. Struct. Theochem*, **4**, 1 (1982).
25. P.E. Sorensen, K. Bruhn, F. Lindelov: *Acta Chem. Scand. Ser. A Phys. Inorg. Chem.*, A**28**, 162 (1974).
26. D.L. Howard, P. Jrgensen, H.G. Kjaergaard: *J. Am. Chem. Soc.*, **127**, 17096 (2005).
27. D.L. Howard, H.G. Kjaergaard: *J. Phys. Chem. A*, **110**, 10245 (2006).
28. T. Scharge, D. Luckhaus, M.A. Suhm: *Chem. Phys.*, **346**, 167 (2008).
29. R.A. Back, S. Yamamoto: *Can. J. Chem.*, **63**, 542 (1985).
30. B. Bakri, J. Demaison, L. Margules, H. Mollendal: *J. Mol. Spectr.*, **208**, 92 (2001).
31. M.E.S. Dunn, G.C. Vaida: V.: *J. Phys. Chem. A*, submitted, (2008).
32. T.L. Eliason, D.K. Havey, V. Vaida: *Chem. Phys. Lett.*, **402**, 239 (2005).
33. N. Rontu, V. Vaida: *J. Mol. Spectr.*, **237**, 19 (2006).
34. N. Rontu, V. Vaida: *J. Phys. Chem. B*, **112**, 276 (2008).
35. K.L. Plath, K. Takahashi, R.T. Skodje, V. Vaida: *J. Phys. Chem. A*, DOI: 10.1021/jp810687t, (2009).
36. A.D. Becke: *J. Chem. Phys.*, **98**, 5648 (1993).
37. C.T. Lee, W.T. Yang, R.G. Parr: *Phys. Rev. B*, **37**, 785 (1988).
38. T. Clark, J. Chandrasekhar, G.W. Spitznagel, P.V. Schleyer: *J. Comp. Chem.*, **4**, 294 (1983).
39. M.J. Frisch, J.A. Pople, J.S. Binkley: *J. Chem. Phys.*, **80**, 3265 (1984).
40. M.J. Frisch, G.W. Trucks, H.B. Schlegel, G.E. Scuseria, M.A. Robb, J.R. Cheeseman, J.A. Montgomery, T. Vreven, K.N. Kudin, J.C. Burant, J.M. Millam, S.S. Iyengar, J. Tomasi, V. Barone, B. Mennucci, M. Cossi, G. Scalmani, N. Rega, G.A. Petersson, H.

Nakatsuji, M. Hada, M. Ehara, K. Toyota, R. Fukuda, J. Hasegawa, M. Ishida, T. Nakajima, Y. Honda, O. Kitao, H. Nakai, M. Klene, X. Li, J.E. Knox, H.P. Hratchian, J.B. Cross, V. Bakken, C. Adamo, J. Jaramillo, R. Gomperts, R.E. Stratmann, O. Yazyev, A.J. Austin, R. Cammi, C. Pomelli, J.W. Ochterski, P.Y. Ayala, K. Morokuma, G.A. Voth, P. Salvador, J.J. Dannenberg, V.G. Zakrzewski, S. Dapprich, A.D. Daniels, M.C. Strain, O. Farkas, D.K. Malick, A.D. Rabuck, K. Raghavachari, J.B. Foresman, J.V. Ortiz, Q. Cui, A.G. Baboul, S. Clifford, J. Cioslowski, B.B. Stefanov, G. Liu, A. Liashenko, P. Piskorz, I. Komaromi, R.L. Martin, D.J. Fox, T. Keith, M.A. Al-Laham, C.Y. Peng, A. Nanayakkara, M. Challacombe, P.M.W. Gill, B. Johnson, W. Chen, M.W. Wong, C. Gonzalez, J.A. Pople, *Gaussian03*; C.02 ed.; Gaussian Inc.: Wallingford CT, 2004; Vol. 110.

41. R. Krishnan, J.S. Binkley, R. Seeger, J.A. Pople: *J. Chem. Phys.*, **72**, 650 (1980).
42. A.D. McLean, G.S. Chandler: *J. Chem. Phys.*, **72**, 5639 (1980).
43. H. Yoshida, A. Ehara, H. Matsuura: *Chem. Phys. Lett.*, **325**, 477 (2000).
44. K. Takahashi, K.L. Plath, V. Vaida, R.T. Skodje: *J. Phys. Chem. A*, **112**, 7321 (2008).
45. K.L. Plath, K. Takahashi, J.L. Axson, G.C. Nelson, R.T. Skodje, V. Vaida: *J. Phys. Chem. A*, In preparation, (2009).
46. D.K. Havey, K.J. Feierabend, K. Takahashi, R.T. Skodje, V. Vaida: *J. Phys. Chem. A*, **110**, 6439 (2006).
47. A. Limbeck, H. Puxbaum, L. Otter, M.C. Scholes: *Atmos. Environ.*, **35**, 1853 (2001).
48. C.J. Hennigan, M.H. Bergin, J.E. Dibb, R.J. Webber: *Geophys. Res. Lett.*, **35**, L18801 (2008).
49. K.E. Altieri, A.G. Carlton, H.J. Lim, B.J. Turpin, S.P. Seitzinger: *Environ. Sci. Technol.*, **40**, 4956 (2006).